Three Novel Polymeric Frameworks Assembled from Cd^{II}, Co^{II}, and Mn^{II} with the Mixed Organic Ligands 3,4-Pyridinedicarboxylate, 1,3-Bis(4-pyridyl)propane, or 1,2-Bis(4-pyridyl)ethane

Zhi-Yong Fu,[a] Sheng-Min Hu,[a] Jing-Cao Dai,[a] Jian-Jun Zhang,[a] and Xin-Tao Wu*[a]

Keywords: Coordination polymer / Crystal engineering / Mixed ligands / Structural topology

Hydrothermal reactions of Cd^{II}, Co^{II}, and Mn^{II} with the mixed ligands 3,4-pyridinedicarboxylate (pydc), 1,3-bis(4-pyridyl)propane (bpp), or 1,2-bis(4-pyridyl)ethane (bpe) gave crystals of $\{[Cd(pydc)(bpp)]\cdot 0.5H_2O\}_n$ (**1**), $\{[Co(pydc)(H_2O)(bpe)_{0.5}]\cdot 0.5H_2O\}_n$ (**2**), and $\{[Mn(pydc)(H_2O)(bpe)_{0.5}]\cdot 0.5H_2O\}_n$ (**3**), respectively. Single-crystal X-ray analyses reveal that these are all three-dimensional non-interpenetrating coordination polymers. Their structures alter markedly with the conformation and the function of the ligands. In **1**, the 3,4-pyridinedicarboxylate acted as a three-connector, a coordination topology of the type (3,5) [containing 3 and 5 connected centers] being generated through self-assembly, while in **2** and **3**, with the help of the four-connector 3,4-pyridinedicarboxylate and the terminal ligand water molecule, another three-dimensional framework with a coordination topology of the type (**4**, **5**) was obtained.

(© Wiley-VCH Verlag GmbH & Co. KGaA, 69451 Weinheim, Germany, 2003)

Introduction

The design and construction of coordination polymers are of great interest due to their intriguing new structural topologies and potential applications as functional materials.[1−6] Many attractive networks with various structural motifs, including honeycomb,[7−8] brick wall,[9] rectangular grid,[10−11] bilayer,[12−15] ladder,[16−17] herringbone,[18] diamondoid,[19−21] and octahedral[22−23] geometries, have been constructed in the past decade by use of single bridging organic ligands such as 4,4′-bipyridine, pyrazine, and related species. Recently, in order to fabricate more novel complicated supramolecular networks, the employment of metal ions with different kinds of organic ligands has gradually become established as a useful strategy.[24−25] This method may provide new structural motifs not accessible by the application of metal ions with a single ligand. The structural and functional features of the whole self-assembled entities contain the information of their components.[26] To date, however, there has been only one reported polymer with pydc as ligand,[27] and no frameworks constructed by it together with other organic ligands have been observed. This paper reports the synthesis and characterization of three new coordination polymers assembled from metal ions and the mixed ligands 3,4-pyridinedicarboxylate, 1,3-bis(4-pyridyl)propane, or 1,2-bis(4-pyridyl)ethane: namely $\{[Cd(pydc)(bpp)]\cdot 0.5H_2O\}_n$ (**1**), $\{[Co(pydc)(H_2O)(bpe)_{0.5}]\cdot 0.5H_2O\}_n$ (**2**), and $\{[Mn(pydc)(H_2O)(bpe)_{0.5}]\cdot 0.5H_2O\}_n$ (**3**) [pydc = 3,4-pyridinedicarboxylate, bpp = 1,3-bis(4-pyridyl)propane, bpe = 1,2-bis(4-pyridyl)ethane]. Single-crystal X-ray analyses show that the conformations and the functions of the ligands play an important role in affecting the final structural motifs of the polymers. In **1,** with 3,4-pyridinedicarboxylic acid acting as a tritopic subunit and 1,3-bis(4-pyridyl)propane acting as a ditopic subunit, the self-assembly results in an interesting three-dimensional framework with a coordination topology of the (3,5) type, while in **2** and **3**, with 3,4-pyridinedicarboxylic acid acting as a tetratopic subunit, 1,2-bis(4-pyridyl)ethane acting as a ditopic subunit, and a water molecule acting as terminal ligand, another appealing three-dimensional framework with a coordination topology of the (4,5) type is obtained. To the best of our knowledge, these are two new, previously unreported types of structural motifs.

Results and Discussion

Syntheses

In the synthesis of **1**, a molar ratio of 2:2:1 (Cd/pydc/bpp) was used in the preparation, but a framework with a stoichiometric ratio of 1:1:1 was obtained. In order to investigate what would happen if the latter ratio was applied, more experiments were done, but unfortunately no single crystal was obtained. When Co^{II} and Mn^{II} were used to repeat the above experimental procedure, complexes **2**

---

[a] State Key Laboratory of Structural Chemistry, Fujian Institute of Research on the Structure of Matter, Chinese Academy of Sciences,
Fuzhou, Fujian 350002, China
Fax: (internat.) + 86-591/3714946
E-mail: wxt@ms.fjirsm.ac.cn

© 2003 Wiley-VCH Verlag GmbH & Co. KGaA, Weinheim DOI: 10.1002/ejic.200300018

and **3**, with 2:2:1 stoichiometric ratios exactly the same as those of the original reactants, were generated.

Crystal Structures

Single-crystal X-ray analysis reveals that **1** has a three-dimensional, non-interpenetrating coordination network. Each Cd^{II} center has a slightly distorted {CdN_3O_4} pentagonal bipyramid coordination sphere, with one 1,3-bis(4-pyridyl)propane nitrogen donor and four oxygen donors of two chelating bidentate carboxylate groups of the 3,4-pyridinedicarboxylate in the equatorial plane. The coordination sphere is completed by one nitrogen donor of 1,3-bis(4-pyridyl)propane and one nitrogen donor of 3,4-pyridinedicarboxylate in the axial direction (Figure 1). The metal centers provide the penta-connecting trigonal bipyramid nodes, while the ligands act as di-connectors and tri-connectors, respectively. The spontaneous association of these subunits results in a new kind of 3D framework (Figure 2, a). In a side view of the network (Figure 2, b), it is interesting to observe that two kinds of rings exist. One is a cyclohexane-like ring, made up of three Cd^{II} ions and three centers of 3,4-pyridinedicarboxylate, displaying a chair conformation, while the other is also a six-membered ring, formed by four Cd^{II} ions and two centers of the 3,4-pyridinedicarboxylate, exhibiting a boat conformation. Viewed onto the *ac* plane, the whole feature of the framework looks like the bellows of an accordion, showing folds. The metal centers, which are distributed in the sheets, are not all coplanar. Rather, half fall in one plane, and half in an adjacent plane, displaying a helical conformation. Two rods of the 1,3-bis(4-pyridyl)propane two-connectors form two edges of the sheet and two rods of the 3,4-pyridinedicarboxylate tri-connectors make up the other edges (connections between nodes within the structure are referred to in general as rods). The third rod of 3,4-pyridinedicarboxylate links to the adjacent layer, producing a remarkable three-dimensional framework. Infinite narrow channels exist in the framework and their arrangement fits the symmetry of the space group *C*2/*c*. The height of one channel is exactly the width of another and each pair of diagonal channels displays a centrosymmetric configuration. Close examination of the channels revealed that water molecules acting as guests were embedded in the cavities and formed hydrogen bonds with the framework (O2···O5 2.776 Å).

Compounds **2** and **3** have the same structural motif, except for the difference in the metal center (Co for **2**, Mn for **3**). The local coordination geometry around the centrosymmetric metal center can be described as a slightly distorted octahedron configuration (Figure 3). One nitrogen atom of the 3,4-pyridinedicarboxylate and one nitrogen atom of 1,2-bis(4-pyridyl)ethane occupy the axial positions of the coordination sphere. Three oxygen atoms of 3,4-pyridinedicarboxylate and one oxygen atom of a water molecule coordinate the metal center in the equatorial plane. What is different from **1** is that two kinds of coordination modes exist in the carboxylate groups of the 3,4-pyridinedicarboxylate in **2** and **3** (Scheme 1). One is bidentate and the other is monodentate, which makes the 3,4-pyridinedicarboxylate ligands act as tetra-connectors. While the water molecule acting as a terminal ligand occupies one reaction site of the octahedral coordination sphere, this makes the six-coordinate metal center also provide a penta-connecting node. Nevertheless, it has a tetragonal pyramid configuration, different from the penta-connecting trigonal bipyramid conformation existing in **1**. The self-assembly of the tetra-connectors and the penta-connecting nodes creates a two-dimensional layer (Figure 4, a). Viewed down the *b* axis, the metal centers of the dinuclear units, located in the layer, are distributed in two different planes (Figure 4, b). The di-connector 1,2-bis(4-pyridyl)ethane occupies the other two reaction sites of the penta-connecting nodes and links the adjacent metal double layers from top and bottom, extending the structural motif into three dimensions (Figure 5). Just as in **1**, the water molecule is also enclathrated in the small cavity of the framework and it also forms a hydrogen bond with its host (O4···O6 2.743Å for **2** and O4···O6 2.819Å for **3**).

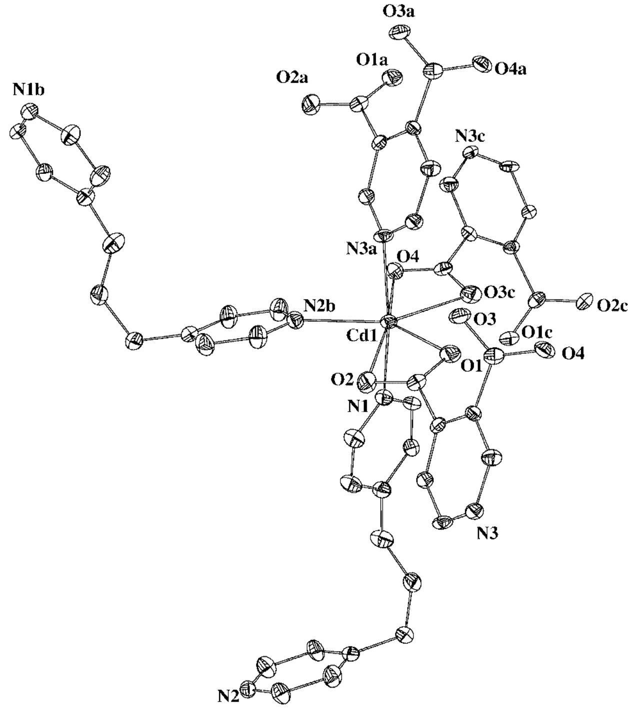

Figure 1. ORTEP drawing (at 30% probability) of **1** around the Cd center; the hydrogen atoms are omitted for clarity; symmetry code: a = *x*, −1 + *y*, *z*; b = 3/2 − *x*, −1 + *y*, 1/2 + *z*; c = 1 − *x*, 2 − *y*, −1/2 + *z*

Carboxylate ligands (such as trimesate, terephthalate, pydc etc.) have a great ability to construct coordination architectures with metal ions, adopting several different coordination fashions, ranging from unidentate to bidentate, sometimes in more than one way in the coordination architecture[28] Their bridging modes are highly dependent on the coordination modes of the carboxy groups, which can affect the final structural motifs of the polymers.[29] In compound **1**, in which the carboxy groups have a chelating bidentate coordination mode, the pydc ligands act as tri-connectors and connect the Cd centers, forming parts of the

© 2003 Wiley-VCH Verlag GmbH & Co. KGaA, Weinheim

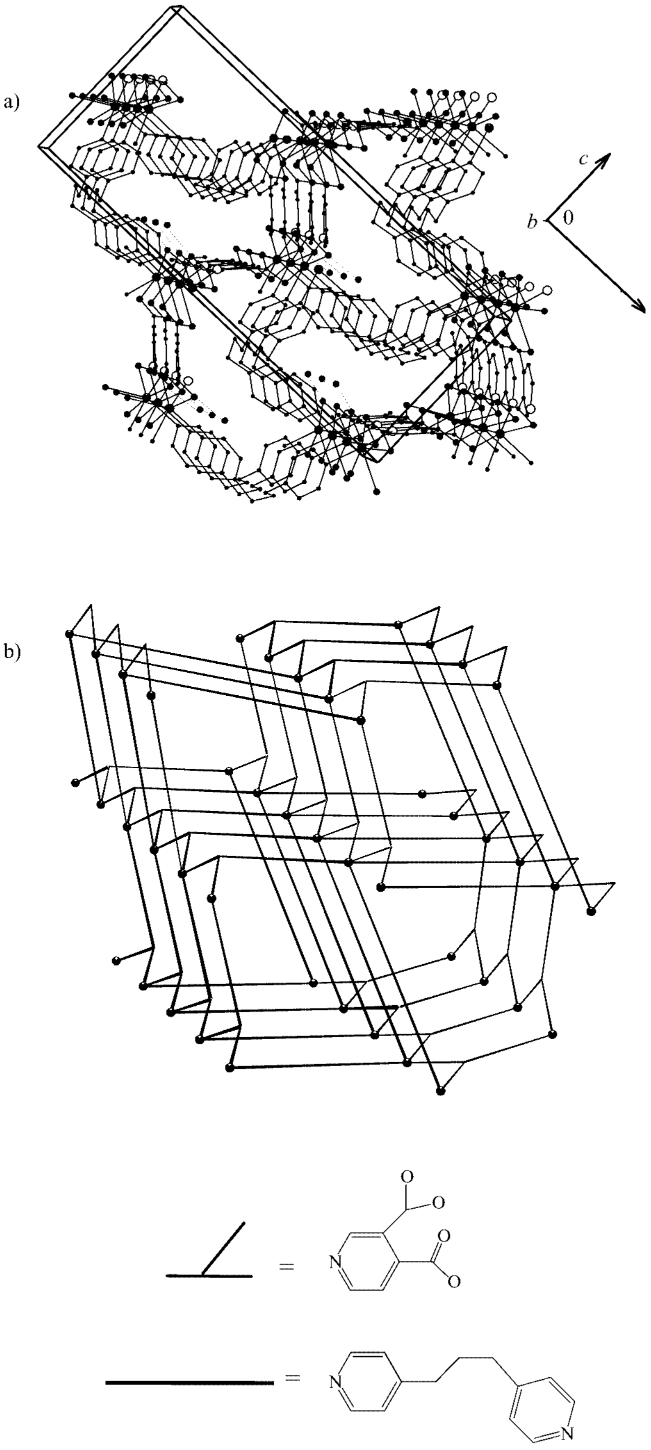

Figure 2. (a) View of the extended structure of **1**, showing the building blocks aggregated to a three-dimensional framework with a coordination topology of the type (3,5); (b) view of the topology of ring linkage in the framework; the close circles symbolize the Cd^{II} ions

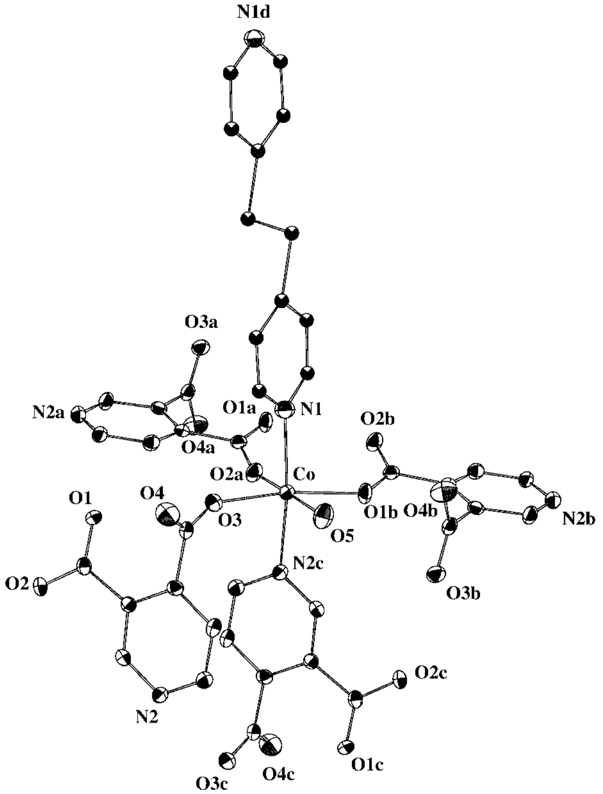

Figure 3. ORTEP drawing (at 30% probability) of **2** around the Co center; the hydrogen atoms are omitted for clarity; the structure of compound **3** is analogous; symmetry code: a = $-x + 1/2$, $y + 1/2$, $-z + 1/2$; b = x, $-y$, $z + 1/2$; c = $-x + 1/2$, $-y - 1/2$, $-z + 1$

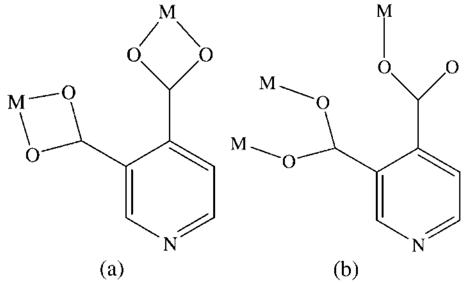

Scheme 1. The coordination fashions of the carboxylate group: (a) compound **1**: chelating bidentate; (b) compounds **2** and **3**: bi- and monodentate

rings, while in compounds **2** and **3** the bi- and monodentate coordination modes make the pydc act as tetra-connectors, which interlock the M (Co, Mn) centers, resulting in M(pydc) layers. The water molecule in **2** and **3** acting as an end-capping unit, also plays an important role affecting the structural feature of the polymers, which making the hexacoordinate metal center provide a penta-connecting node. The whole structural feature of a coordination architecture results from the conformation of ligand and the coordination mode of metal center.[30–31] Different metal coordination geometries and different orientations of the interaction sites in a given ligand cause the framework to display various structural motifs.

Thermal Stability

To study the stability of these materials, thermogravimetric analyses (TGA) were performed on polycrystalline samples of these three compounds. The data for **1** showed

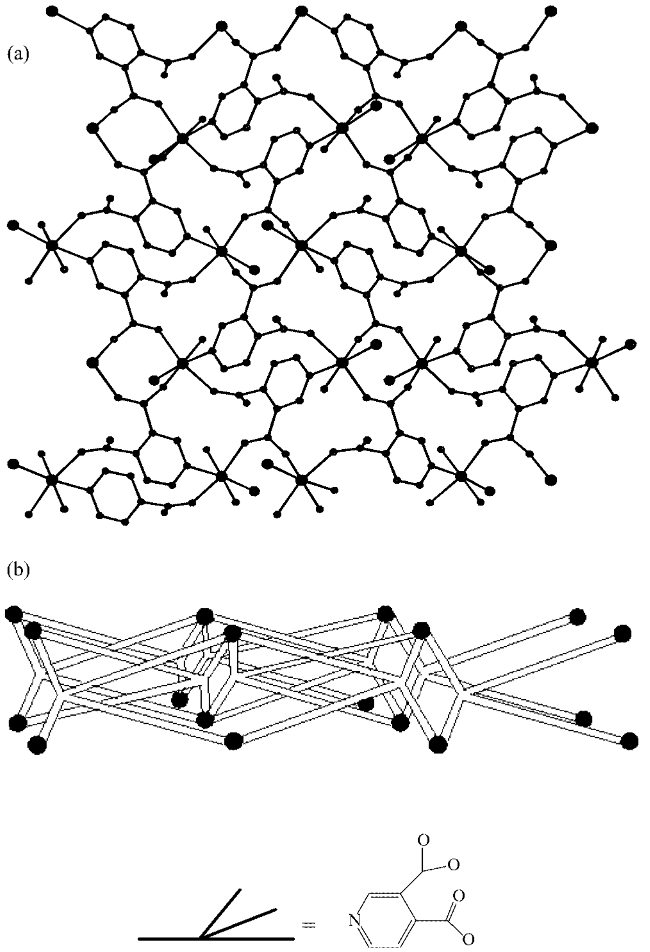

Figure 4. (a) View of the two-dimensional layer connected by the 3,4-pyridinedicarboxylate ligands in **2** from the *a* direction; (b) a schematic view of the two-dimensional layer from the *b* direction

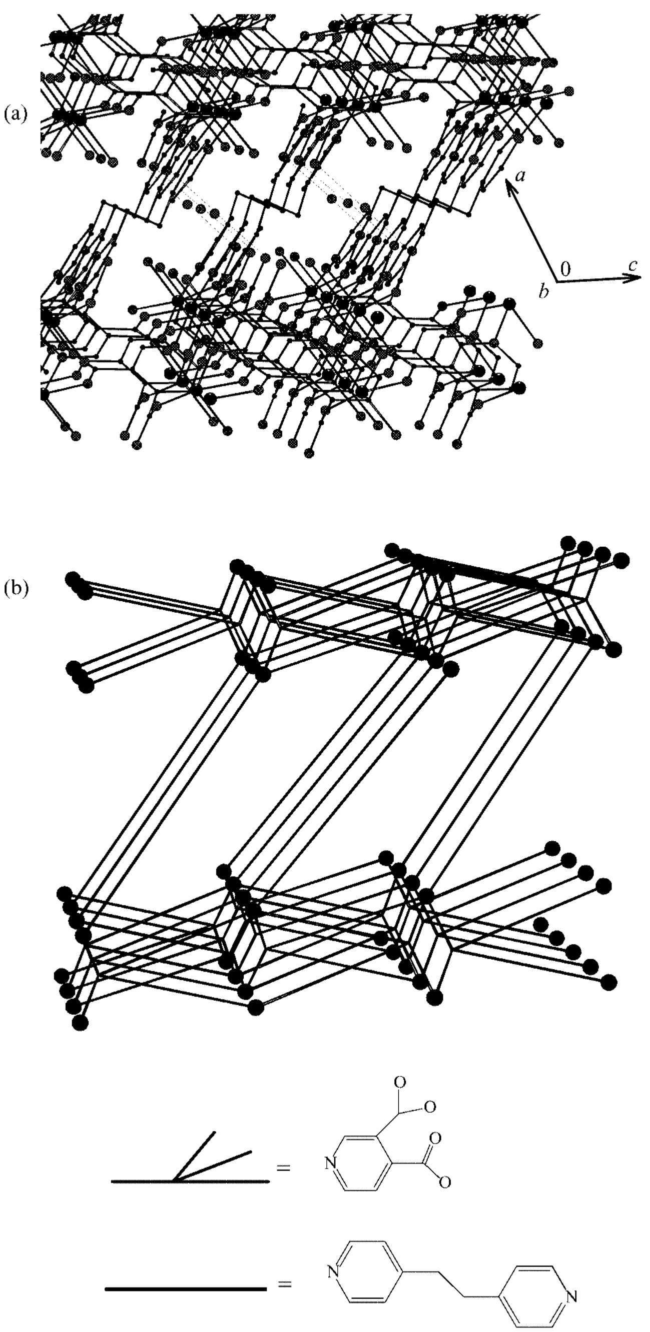

Figure 5. (a) View of the extended structures of **2**, showing the building blocks aggregated into a three-dimensional framework with a coordination topology of the (4,5) type; (b) view of the topology of ring linkage in the framework; the close circles symbolize the metal centers (M = Co and Mn for **2** and **3**, respectively)

the two following, strikingly clean and well-separated, weight loss steps. In the first region (100−130 °C), it lost all guest water molecules (2% observed, 1.86% calculated). On further heating, the material lost weight continuously, corresponding to the preliminary decomposition of the whole framework, and an obvious decomposition was observed at 300 °C, corresponding to the final decomposition of the whole framework (Figure 6, a). The thermal decomposition behavior of compounds **2** and **3** was similar. The first weight loss in **2** started at ca. 105 °C up to 150 °C to give a weight loss of ca. 3%, corresponding to the loss of the solvated water molecule (2.62% calculated). On further heating, it lost one coordinated water molecule per formula unit between 150 °C and 250 °C (5.4% observed, 5.25% calculated). Immediately above 250 °C, an obvious weight loss continuing to 290 °C was observed, corresponding to the loss of half a bpe molecule per formula unit (27.4% observed, 26.84% calculated). The decomposition of **2** was complete at ca. 500 °C (Figure 6, b). In compound **3**, an initial weight loss of 2.7% at 150 °C, corresponding to the removal of the solvated water molecule (2.65% calculated), was followed by further weight loss of 5.92% (5.31% calculated) at 305 °C for evacuation of the coordinated water molecule. From 305 to 350 °C, the TGA trace of **3** showed a sharp decline to give a total weight loss of ca. 28.3% (27.16% calculated), corresponding to the loss of half a bpe molecule per formula unit. Finally, compound **3** decomposed completely at about 510 °C (Figure 6, c). All TGA data indicate that the guest water molecules play an important role in stabilizing these coordination networks. When these are liberated from the cavities, the frameworks im-

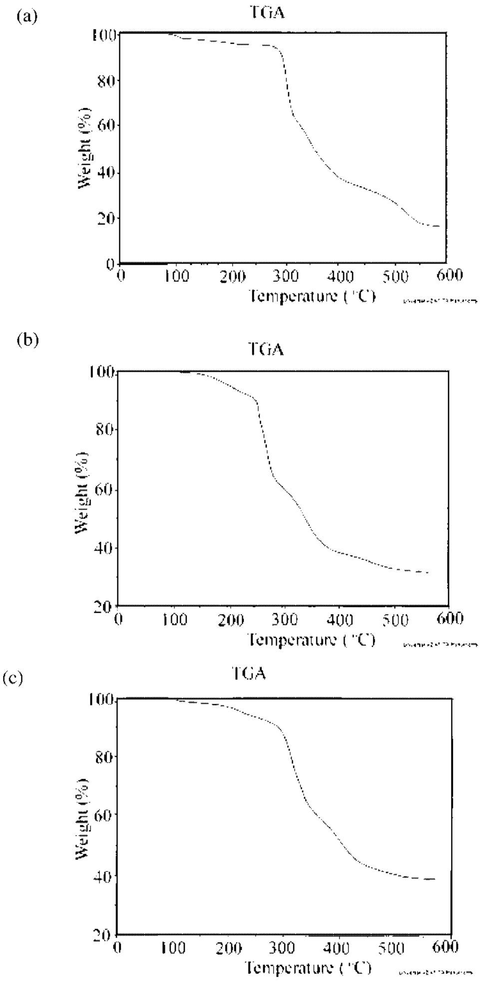

Figure 6. TGA diagram for the coordination polymers: (*a*) compound **1**; (*b*) compound **2**; (c) compound **3**

mediately begin to collapse. The corresponding X-ray powder diffraction (XRPD) data also confirm these changes (Figure 7).

Fluorescent Properties

The emission spectra of complexes **1**–**3** in the solid state at room temperature are shown in Figure 8. It can be observed that the intense emissions occurring in the same range for the three different metals can be assigned to ligand-metal charge-transfer (LMCT) bands, similar to those observed for dipyridinocrown ether ligands[32] (Figure 8, a: λ_{ex} = 210 nm, λ_{em} = 326 nm for **1**; Figure 8, b: λ_{ex} = 300 nm, λ_{em} = 398 nm for **2**; Figure 8, c: λ_{ex} = 220 nm, λ_{em} = 350 nm for **3**). Interestingly, a weak emission occurring at 486 nm for **2** (Figure 8, b: λ_{ex} = 300 nm), assigned as metal-ligand charge-transfer (MLCT) band, can be also observed. The reason for the MLCT phenomenon only occurring in compound **2** and not in compounds **1** and **3** may be that compound **2** contains the d^7 Co^{2+} metal center, in which d-electronic transition is easier than in the d^{10} Cd^{2+} metal center and in the d^5 Mn^{2+} metal center in the other two compounds.

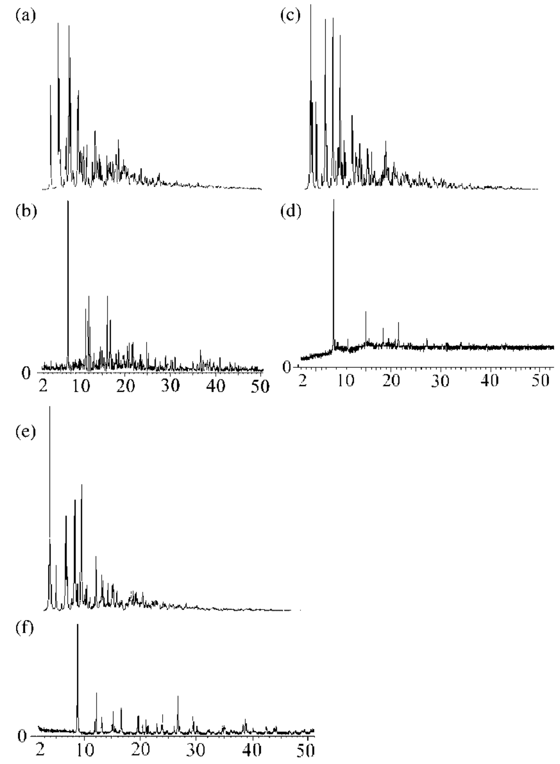

Figure 7. X-ray diffraction pattern for: (a) **1**, as synthesized; (b) solid of **1** heated at 130 °C for 2 h; (c) **2**, as synthesized; (d) solid of **2** heated at 150 °C for 2 h; (e) **3**, as synthesized; (f) solid of **3** heated at 150 °C for 2 h

Conclusion

Three new coordination polymers have been obtained by self-assembly of Cd^{II}, Co^{II}, and Mn^{II} with the mixed ligands 3,4-pyridinedicarboxylate (pydc), 1,3-bis(4-pyridyl)propane (bpp), or 1,2-bis(4-pyridyl)ethane (bpe). The stabilities of these compounds are dependent on the existence of their guest molecules; when these guest molecules are liberated, the frameworks collapse. The structural figures of these whole frameworks contain the information of their components. In **1**, the penta-connecting trigonal bipyramid nodes combining with the di- and tri-connectors result in a (3,5) connected framework, while in **2** and **3**, with the penta-connecting tetragonal pyramid nodes cooperating with the di- and tetra-connectors, another interesting (4,5) connected framework was obtained.

This work shows that the conformations and the functions of the ligands play an important role in affecting the final structural motifs of the polymers. Investigation of the different coordination modes of the ligands may also help in the design of novel structural frameworks and fabrication of new functional materials.

Experimental Section

Materials and Methods: All chemicals were purchased and used without further purification. The C, H and N microanalyses were carried out with a Vario EL III elemental analyzer. Infrared spectra

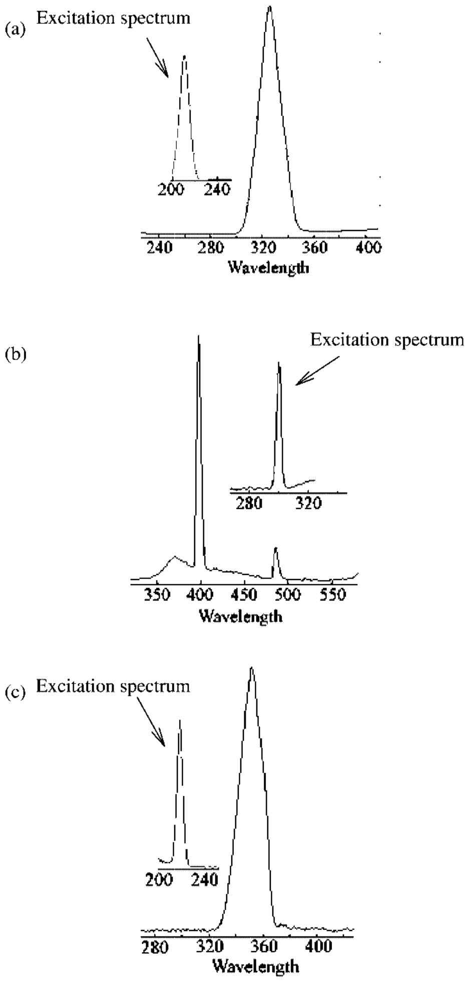

Figure 8. Solid-state emission spectra of the complexes at room temperature: (a) **1**; (b) **2**; (c) **3**

(KBr pellets) were recorded in the 4000−400 cm^{-1} range with a Nicolet Magna 750 FT-IR spectrometer. Thermogravimetric analysis (TGA) was performed under nitrogen with a heating rate of 10 °C·min^{-1} using a TA5200/MDSC2910 system (TA Instruments, Inc.). Fluorescent spectra were measured with an Edinburgh FL-FS90 TCSPC system. X-ray powder diffraction were recorded with a Bruker AXS D8 advanced automated diffractometer with Cu-K_{α} radiation; the sample was heated in air and the measurement was performed after the sample had cooled down to room temperature.

Synthesis of $C_{20}H_{19}CdN_3O_{4.5}$ (1): An aqueous mixture (10 mL) containing 3,4-pyridinedicarboxylic acid (1 mmol), $Cd(NO_3)_2$·$4H_2O$ (1 mmol), 1,3-bis(4-pyridyl)propane (0.5 mmol), and NaOMe (2 mmol) was placed in a Parr Teflon-lined stainless steel vessel (25 mL), and the vessel was sealed and heated to 150 °C for 168 h, then cooled at 2.5 °C h^{-1} to room temperature. Colorless needle-like crystals (0.14 g) were obtained in 56% yield. $C_{20}H_{19}CdN_3O_{4.5}$ (484.77): calcd. C 49.28, H 3.93, N 8.63; found C 48.29, H 3.67, N 8.62. IR (KBr pellet): $\tilde{\nu}$ = 3361 m, 3221 w, 3053 w, 2945 m, 1614 s, 1606 s, 1585 s, 1570 s, 1547 m, 1406 s, 1417 s, 1385 s, 1227 m, 1061 w, 1011 m, 847 s, 814 m, 785 m, 721 m, 683 m, 525 w cm^{-1}.

Synthesis of $C_{13}H_{12}CoN_2O_{5.50}$ (2): An aqueous mixture (10 mL) containing 3,4-pyridinedicarboxylic acid (1 mmol), $Co(NO_3)_2$·$6H_2O$ (1 mmol), 1,2-bis(4-pyridyl)ethane (0.5 mmol), and NaOMe (2 mmol) was placed in a Parr Teflon-lined stainless steel vessel (25 mL), and the vessel was sealed and heated to 150 °C for 168 h, then cooled at 2.5 °C h^{-1} to room temperature. Red block crystals (0.15 g) were obtained in 43% yield. $C_{13}H_{12}CoN_2O_{5.50}$ (343.18): calcd. C 45.50, H 3.52, N 8.16; found C 45.11, H 3.46, N 8.13. IR (KBr pellet): $\tilde{\nu}$ = 3350 m, 3084 w, 2945 w, 1641 s, 1616 m, 1572 s, 1547 s, 1412 s, 1398 s, 1230 w, 1171 w, 1016 w, 816 w, 677 w cm^{-1}.

Synthesis of $C_{13}H_{12}MnN_2O_{5.50}$ (3): An aqueous mixture (10 mL) containing 3,4-pyridinedicarboxylic acid (1 mmol), $MnCl_2$·$4H_2O$ (1 mmol), 1,2-bis(4-pyridyl)ethane (0.5 mmol), and NaOMe(2 mmol) was placed in a Parr Teflon-lined stainless steel vessel (25 mL), and the vessel was sealed and heated to 150 °C for 168 h, then

Table 1. Crystal data and refinement details for the structures of **1**, **2**, and **3**

Complex	**1**	**2**	**3**
Empirical formula	$C_{20}H_{18}CdN_3O_{4.5}$	$C_{13}H_{12}CoN_2O_{5.50}$	$C_{13}H_{12}MnN_2O_{5.50}$
Formula mass	484.77	343.18	339.19
Space group	Pca2(1)	*C*2/*c*	*C*2/*c*
a [Å]	24.5356(10)	23.2508(1)	23.001(2)
b [Å]	7.6283(2)	10.9695(3)	11.2151(11)
c [Å]	10.5098(4)	11.5021(2)	11.6851(12)
α	90	90	90
β	90	113.609(1)	112.971(2)
γ	90	90	90
V [$Å^3$]	1967.07(12)	2688.06(9)	2775.3(5)
Z	4	8	8
μ(Mo-K_{α}) [mm^{-1}]	1.144	1.305	0.979
θ range [°]	1.66−25.06	1.91−25.04	1.92−25.04
$d_{calcd.}$ [g/cm^3]	1.637	1.696	1.624
Final *R* indices [$I > 2\sigma(I)$][a]	$R1 = 0.0405$ $wR2 = 0.0712$	$R1 = 0.0476$ $wR2 = 0.1110$	$R1 = 0.0608$ $wR2 = 0.1342$
Max/mean shift in final cycle	0.000/0.000	0.000/0.000	0.000/0.000
Maximum/minimum ρ [e×$Å^{-3}$]	0.657/−0.636	0.617/−0.675	0.631/−0.475

[a] $R = \Sigma(||F_o| - |F_c||)/\Sigma\,|F_o|$; $wR = \{\Sigma w[(F^2{}_o - F^2{}_c)]/\Sigma w[(F^2{}_o)^2]\}^{0.5}$; $w = [\sigma^2(F^2{}_o) + (0.0283P)^2 + 0.0000P]^{-1}$ for compound **1**, $w = [\sigma^2(F^2{}_o) + (0.0523P)^2 + 13.5832P]^{-1}$ for compound **2**, and $w = [\sigma^2(F^2{}_o) + (0.0546P)^2 + 21.5163P]^{-1}$ for compound **3**, where $P = (F^2{}_o + 2F^2{}_c)/3$.

© 2003 Wiley-VCH Verlag GmbH & Co. KGaA, Weinheim

Table 2. Selected bond lengths [Å] and bond angles [°] for **1**, **2**, and **3**; symmetry codes: a = $-x + 3/2$, $y - 1$, $z + 1/2$; b = x, $y - 1$, z; c = $-x + 1$, $-y + 2$, $z - 1/2$ for **1**; a = $-x + 1/2$, $y + 1/2$, $-z + 1/2$; (b) x, $-y$, $z + 1/2$; c = $-x + 1/2$, $-y - 1/2$, $-z + 1$ for **2** and **3**

{[Cd(pydc)(bpp)]·0.5H_2O}$_n$ (**1**):			
Cd(1)−N(1)	2.347(6)	Cd(1)−O(4c)	2.390(6)
Cd(1)−O(1)	2.351(5)	Cd(1)−O(3c)	2.496(5)
Cd(1)−N(2a)	2.381(4)	Cd(1)−O(2)	2.524(6)
Cd(1)−N(3b)	2.382(7)		
N(1)−Cd(1)−O(1)	98.47(19)	N(2a)−Cd(1)−O(3c)	139.2(2)
N(1)−Cd(1)−N(2a)	83.3(3)	N(3b)−Cd(1)−O(3c)	90.5(2)
O(1)−Cd(1)−N(2a)	138.2(2)	O(4c)−Cd(1)−O(3c)	53.47(18)
N(1)−Cd(1)−N(3b)	169.4(2)	N(1)−Cd(1)−O(2)	87.2(2)
O(1)−Cd(1)−N(3b)	92.1(2)	O(1)−Cd(1)−O(2)	53.85(17)
N(2a)−Cd(1)−N(3b)	89.6(3)	N(2a)−Cd(1)−O(2)	84.7(2)
N(1)−Cd(1)−O(4c)	88.3(2)	N(3b)−Cd(1)−O(2)	100.1(2)
O(1)−Cd(1)−O(4c)	135.6(2)	O(4c)−Cd(1)−O(2)	170.2(2)
N(2a)−Cd(1)−O(4c)	86.1(2)	O(3c)−Cd(1)−O(2)	135.12(17)
N(3b)−Cd(1)−O(4c)	83.4(2)	O(1)−Cd(1)−O(3c)	82.53(16)
N(1)−Cd(1)−O(3c)	89.73(19)		
{[Co(pydc)(H_2O)(bpe)$_{0.5}$]·0.5H_2O}$_n$ (**2**):			
Co(1)−O(2a)	2.037(3)	Co(1)−O(5)	2.157(3)
Co(1)−O(1b)	2.077(3)	Co(1)−N(1)	2.166(3)
Co(1)−O(3)	2.108(3)	Co(1)−N(2c)	2.168(3)
O(2a)−Co(1)−O(1b)	98.46(11)	O(3)−Co(1)−N(1)	87.95(12)
O(2a)−Co(1)−O(3)	95.29(11)	O(5)−Co(1)−N(1)	92.08(13)
O(1b)−Co(1)−O(3)	165.53(11)	O(2a)−Co(1)−N(2c)	85.06(12)
O(2a)−Co(1)−O(5)	178.63(12)	O(1b)−Co(1)−N(2c)	88.25(12)
O(1b)−Co(1)−O(5)	81.13(11)	O(3)−Co(1)−N(2c)	88.50(12)
O(3)−Co(1)−O(5)	85.02(12)	O(5)−Co(1)−N(2c)	93.62(12)
O(2a)−Co(1)−N(1)	89.26(13)	N(1)−Co(1)−N(2c)	173.00(13)
O(1b)−Co(1)−N(1)	96.65(12)		
Co(1)−O(2a)	2.037(3)	Co(1)−O(5)	2.157(3)
Co(1)−O(1b)	2.077(3)	Co(1)−N(1)	2.166(3)
Co(1)−O(3)	2.108(3)	Co(1)−N(2c)	2.168(3)
{[Mn(pydc)(H_2O)(bpe)$_{0.5}$]·0.5H_2O}$_n$ (**3**):			
Mn(1)−O(2a)	2.117(4)	Mn(1)−O(3)	2.161(3)
Mn(1)−O(1b)	2.144(3)	Mn(1)−N(2c)	2.301(4)
Mn(1)−O(5)	2.225(4)	Mn(1)−N(1)	2.290(4)
O(2a)−Mn(1)−O(1b)	99.52(14)	O(5)−Mn(1)−N(2c)	96.86(15)
O(2a)−Mn(1)−O(5)	179.49(14)	O(3)−Mn(1)−N(2c)	86.56(14)
O(1b)−Mn(1)−O(5)	79.97(14)	O(2a)−Mn(1)−N(1)	88.27(15)
O(2a)−Mn(1)−O(3)	95.39(14)	O(1b)−Mn(1)−N(1)	99.22(15)
O(1b)−Mn(1)−O(3)	163.24(14)	O(5)−Mn(1)−N(1)	91.76(16)
O(5)−Mn(1)−O(3)	85.12(14)	O(3)−Mn(1)−N(1)	88.79(14)
O(2a)−Mn(1)−N(2c)	83.16(14)	N(2c)−Mn(1)−N(1)	169.81(16)
O(1b)−Mn(1)−N(2c)	87.65(14)		

cooled at 2.5 °C h^{-1} to room temperature. Yellow block crystals (0.14 g) were obtained in 41% yield. $C_{13}H_{12}MnN_2O_{5.50}$ (339.19): calcd. C 46.03, H 3.57, N 8.26; found C 46.21, H 3.33, N 8.22. IR (KBr pellet): $\tilde{\nu}$ = 3358 s, 3055 m, 2945 w, 1637 s, 1614 s, 1576 s, 1547 s, 1414 s, 1398 s, 1228 m, 1012 m, 818 m, 675 m cm^{-1}.

X-ray Crystallographic Study: Crystallographic data for compounds **1**, **2**, and **3** are listed in Table 1. Data for **1**, **2**, and **3** were collected at room temperature with a Siemens SMART-CCD area-detector diffractometer with Mo-K_α radiation (λ = 0.71073 Å) and graphite monochromator using the ω-scan mode. Data reductions and absorption corrections were performed with SMART and SADABS software, respectively. The structures were solved by direct methods by use of SHELXS-97[33] and refined on F^2 by full-matrix, least squares.[34] All non-hydrogen atoms were treated anisotropically. The positions of hydrogen atoms were generated geometrically. The selected bond lengths and bond angles for the cluster cores of **1**, **2**, and **3** are listed in Table 2. CCDC-196855 to -196857 contain the supplementary crystallographic data for this paper. These data can be obtained free of charge at www.ccdc.cam.ac.uk/conts/retrieving.html [or from the Cambridge Crystallographic Data Centre, 12 Union Road, Cambridge CB2 1EZ, UK; Fax: (internat.) + 44-1223/336-033; E-mail: deposit@ccdc.cam.ac.uk].

Acknowledgments

This work is supported by grants from the State Key Laboratory of Structural Chemistry, Fujian Institute of Research on the Structure of Matter, the Chinese Academy of Sciences (CAS), and also the Ministry of Science and Technology of China (001CB1089), the National Science Foundation of China (20273073, 90206040), and the Science Foundation of CAS and Fujian Province, for research funding support (2002F014). Z.-Y. F. and J.-C. D. wish to thank Dr. J.-M. Lin for the PRXD determination and Prof. W.-D. Cheng for useful discussions on fluorescent properties.

---

[1] S. R. Batten, R. Robson, *Angew. Chem. Int. Ed.* **1998**, *37*, 1460−1494.
[2] M. J. Zaworotko, *Chem. Soc. Rev.* **1994**, 283−288.

[3] P. J. Hagrman, D. Hagrman, J. Zubieta, *Angew. Chem. Int. Ed.* **1999**, *38*, 2639−2684.
[4] S. Noro, S. Kitagawa, M. Kondo, K. Seki, *Angew. Chem. Int. Ed.* **2000**, *39*, 2081−2084.
[5] M. Kondo, T. Yoshitomi, K. Seki, H. Matsuzaka, S. Kitagawa, *Angew. Chem. Int. Ed. Engl.* **1997**, *36*, 1725−1727.
[6] R. Robson, *Comprehensive Supramolecular Chemistry*, Pergamon, England, **1996**, chapter 22, pp. 733−755.
[7] M. Hayashi, Y. Miyamoto, T. Inoue, N. Oguni, *J. Chem. Soc., Chem. Commun.* **1991**, 1752−1753.
[8] G. B. Gardner, D. Venkataraman, J. S. Moore, S. Lee, *Nature* **1995**, *374*, 792−795.
[9] R. W. Gable, B. F. Hoskins, R. Robson, *J. Chem. Soc., Chem. Commun.* **1990**, 1677−1678.
[10] M. Fujita, Y. J. Kwon, S. Washizu, K. Ogura, *J. Am. Chem. Soc.* **1994**, *116*, 1151−1152.
[11] L. R. MacGillivray, R. H. Groeneman, J. L. Atwood, *J. Am. Chem. Soc.* **1998**, *120*, 2676−2677.
[12] M. Kondo, T. Yoshitomi, K. Seki, H. Matsuzaka, S. Kitagawa, *Angew. Chem. Int. Ed. Engl.* **1997**, *36*, 1725−1727.
[13] K. N. Power, T. L. Hennigar, M. J. Zaworotko, *New J. Chem.* **1998**, 177−181.
[14] C. J. Kepert, M. J. Rosseinsky, *Chem. Commun.* **1999**, 375−376.
[15] Z. Y. Fu, X. T. Wu, J. C. Dai, L. M. Wu, C. P. Cui, S. M. Hu, *Chem. Commun.* **2001**: 1856−1857.
[16] P. Losier, M. J. Zaworotko, *Angew. Chem. Int. Ed. Engl.* **1996**, *35*, 2779−2782.
[17] T. L. Hennigar, D. C. MacQuarrie, P. Losier, R. D. Rogers, M. J. Zaworotko, *Angew. Chem. Int. Ed. Engl.* **1997**, *36*, 972−973.
[18] M. A. Withersby, A. J. Blake, N. R. Champness, P. A. Cooke, P. Hubberstey, M. Schroder, *New J. Chem.* **1999**, *23*, 573−575.
[19] L. R. MacGillivray, S. Subramanion, M. J. Zaworotko, *Chem. Commun.* **1994**, 1325−1326.
[20] L. Carlucci, G. Ciani, D. M. Proserpio, A. Sironi, *J. Chem. Soc., Chem. Commun.* **1994**, 2755−2756.
[21] O. M. Yaghi, H. Li, *J. Am. Chem. Soc.* **1995**, *117*, 10401−10402.
[22] T. Soma, H. Yuge, T. lwamoto, *Angew. Chem. Int. Ed. Engl.* **1994**, *33*, 1665−1666.
[23] S. Subramanian, M. J. Zaworotko, *Angew. Chem. Int. Ed. Engl.* **1995**, *34*, 2127−2129.
[24] F. A. Cotton, C. Lin, C. A. Murillo, *Chem. Commun.* **2001**, 11−12.
[25] S. M. Lo, S. Y. Chui, L. Y. Shek, Z. Lin, X. X. Zhang, G. Wen, I. D. Williams, *J. Am. Chem. Soc.* **2000**, *122*, 6293−6294.
[26] S. Leininger, B. Olenyuk, P. J. Stang, *Chem. Rev.* **2000**, *100*, 853−908.
[27] E. E. Sileo, D. Vega, R. Baggio, M. T. Garland, M. A. Blesa, *Aust. J. Chem.* **1999**, *52*, 205−212.
[28] M. Eddaoudi, D. B. Moler, H. Li, B. Chen, T. M. Reineke, M. O'keeffe, O. M. Yaghi, *Acc. Chem. Res.* **2001**, *34*, 319−330.
[29] J. C. Dai, X. T. Wu, Z. Y. Fu, C. P. Cui, S. M. Hu, W. X. Du, L. M. Wu, H. H. Zhang, R. Q. Sun, *Inorg. Chem.* **2002**, *41*, 1391−1396.
[30] S. Leininger, B. Olenyuk, P. J. Stang, *Chem. Rev.* **2000**, *100*, 853−908.
[31] K. N. Power, T. L. Hennigar, M. J. Zaworotko, *New J. Chem.* **1998**, 177−181.
[32] A. Tahri, E. Cielen, K. J. V. Aken, G. J. Hoornaert, F. C. D. Schryver, N. Boens, *J. Chem. Soc., Perkin Trans. 2* **1999**, 1739−1748.
[33] G. M. Sheldrick, *Acta Crystallogr., Sect. A* **1990**, *46*, 467.
[34] G. M. Sheldrick, *SHELXL-97*, *Program for X-ray Crystal Structure Refinement*, University of Göttingen, Göttingen, Germany, **1997**.

Received January 12, 2003

© 2003 Wiley-VCH Verlag GmbH & Co. KGaA, Weinheim